NMR spin grouping and correlation exchange analysis

Application to low hydration NaDNA paracrystals

L. J. Schreiner,* J. C. MacTavish,* M. M. Pintar,* and A. Rupprecht‡

*Department of Physics, University of Waterloo, Waterloo, Ontario, Canada N2L 3G1; and ‡Arrhenius Laboratory, University of Stockholm, Stockholm, Sweden

ABSTRACT The NMR spin-grouping technique is applied to low hydration oriented fibers of NaDNA to study the role of exchange in determining the apparent (observed) spin relaxation of the system. The analysis proceeds in three steps: first, the apparent proton relaxation is measured at high fields, with both selective and nonselective inversion pulse sequences, and in the rotating frame. The spin-grouping technique is used in all spin-lattice relaxation measurements to provide the optimum apparent relaxation characterization of the sample. Next, all apparent results are analyzed for exchange. In this analysis the results from the high field and rotating frame experiments (which probe the exchange at two different time scales) are correlated to determine the inherent (or true) spin relaxation parameters of each of the proton groups in the system. The results of selective inversion T_1 measurements are also incorporated into the exchange analysis. Finally, the dynamics of each spin group are inferred from the inherent relaxation characterization.

The low hydration NaDNA structure is such that the exchange between the protons on the water and those on the NaDNA is limited, a priori, to dipolar mixing. The results of the exchange analysis indicate that the dipolar mixing between water and NaDNA protons is faster than the spin diffusion within the NaDNA proton group itself. The spin-diffusion on the macromolecule is the bottleneck for the exchange between the water protons and the NaDNA protons.

The water protons serve as the relaxation sink both at high fields and in the rotating frame for the total NaDNA-water spin bath. The inherent relaxation of the water is characteristic of water undergoing anisotropic motion with a fast reorientational correlation time about one axis ($5 \times 10^{-10} \leq \tau_r \leq 8 \times 10^{-9}$ s) which is about three orders of magnitude slower than that of water in the bulk; and a slow tumbling correlation time for this axis ($1.5 \times 10^{-7} \leq \tau_t \leq 8 \times 10^{-7}$ s) which is two orders of magnitude slower yet.

INTRODUCTION

Recently, there has been renewed interest in better determining the nuclear magnetic resonance (NMR) relaxation behavior of biological tissue (1, 2). In particular, with the advent of magnetic resonance imaging, it is hoped that this may lead to an improved understanding of tissue relaxation which, in turn, may provide improved tissue characterization for diagnostic purposes. Tissues are heterogeneous systems with protons in a variety of environments, or spin groups, which are not isolated but are mixed by exchange processes. Therefore, the relaxation behavior of tissues depends not only on the inherent relaxation of each spin group, but also on the exchange processes between the groups. It has been realized for some time that the proton spin groups associated with the water in the tissue play a dominant role in determining tissue NMR relaxation parameters. For example, a major model for tissue relaxation is the fast exchange two-state model, in which the system relaxation is determined predominantly by the relaxation of bulk water and bound water spin groups coupled by fast exchange (1–4). Much effort has been undertaken to determine the nature of the structure and the dynamics of the water in the bulk and bound environments. While the details of the models of the water dynamics in these environments may not agree, the premises are that the water in the bulk group is free, i.e., each molecule undergoes fast isotropic reorientation and translation, while the water molecules in the bound environment are hindered so that they are able to reorient anisotropically about one or two axes only. In all such models it is clear that the proton relaxation of the tissue is dominated by the relaxation of the bound water spin group. At high fields the spin-lattice relaxation of tissue in general can be well modeled by assuming fast exchange between the two water environments, so that the water relaxation rate is a weighted average of the relaxation rates of the two groups. However, the spin-lattice relaxation in the rotating frame and the spin–spin relaxation cannot be explained by this model (4–6).

In this paper the results of experiments designed to probe the structure and dynamics of the bound water spin group and the exchange between this spin group and the large molecule spin group are presented. The work was undertaken on hydrated samples of oriented

Dr. Schreiner's present address is Department of Radiation Oncology, McGill University, Montreal, Quebec, Canada.

0006-3495/91/01/221/14 $2.00

sodium salts of deoxyribonucleic acid (NaDNA) because hydrates of macromolecules in the solid state have the advantage that the large molecules are essentially rigid, and the protons on these molecules do not contribute significantly to the magnetic relaxation of the total spin mass.

In addition, a methodology for the analysis of relaxation and exchange of heterogeneous systems is presented. The technique involves determining the apparent proton magnetic relaxation of the system at both high fields (T_1 measurements) and in the rotating frame ($T_{1\rho}$ measurements) using the spin-grouping technique (7, 8), which provides improved resolution of the proton magnetization evolution. Next, all apparent results are analyzed to account for exchange. The exchange analyses at high fields and in the rotating frame are correlated to determine uniquely the inherent relaxation rates of the separate spin groups and the exchange rates between the groups (4, 6, 9). The results of this correlation are reliable because in the present system, as in model biological systems and tissues in general, the $T_{1\rho}$'s are typically an order of magnitude shorter than the T_1's and, therefore, the exchange processes are probed at two time scales. Independent information on exchange is obtained by using the selective inversion NMR pulse sequences at high fields (10).

MATERIALS AND METHODS

The sample of highly oriented sodium NaDNA was prepared by wet spinning (11) Worthington calf-thymus DNA. Care was taken in the preparation of the DNA to avoid contamination of the samples by paramagnetic impurities. The samples contained $<1\%$ NaCl by weight and were in the A form at both water contents studied (12). The single paracrystal of NaDNA had a volume of $\sim 5 \times 5 \times 8$ mm^3 at 75% relative humidity (r.h.). It was placed in a thin walled 8 mm O.D. NMR glass sample tube with the direction of the DNA fiber axes perpendicular to the axis of the sample tube. The water contents of the samples were established by the method of Falk et al. (13): the NaDNA was first exposed to a 33% r.h. atmosphere over aqueous magnesium chloride and the NMR measurements performed; it was then equilibrated in the 49% r.h. atmosphere from saturated aqueous potassium nitrate. The samples were exposed to the controlled r.h. atmosphere for a period of at least 1 wk. The degree of hydration of the NaDNA was confirmed by gravimetric measurements and by NMR FID measurements. The 33% r.h. and the 49% r.h. NaDNA samples contained 3.0 ± 0.5 and 5.0 ± 0.5 mol H_2O per mol nucleotide, respectively.

The apparent proton relaxation times T_1 and T_2 were measured at 21°C with Bruker SXP and CXP spectrometers (Bruker Instruments Ins., Billerica, MA) operating at 40 and 200 MHz, respectively. The relaxation times in the rotating frame, $T_{1\rho}$, were measured using the 40 MHz spectrometer with a spin-locking field pulse of 7 G. The signal averaging and the data analysis were performed with a Hewlett-Packard model 9845 minicomputer (Hewlett-Packard, Palo-Alto, CA) interfaced to the spectrometers through a Biomation 805 transient wave recorder (Biomation Inc., Cupertino, CA). All NMR signals were recorded with an 8-μs delay after the r.f. pulse to account for the deadtime of the receiver of the spectrometer. Typically 100 signals were averaged for each T_2 measurement, while 16 signals were accumulated for each pulse spacing in the spin-lattice relaxation measurements. The T_1's were measured with both selective and nonselective inversion recovery pulse sequences (10). In the nonselective sequence, the inversion pulse was a "hard" pulse of duration 2.4 μs (much less than the T_2 of the solid component of the magnetization) so that the magnetization of all spin groups was inverted. For the "soft" pulse sequence, the inversion pulse duration was typically 80–100 μs, greater than the T_2 of the solid component of the magnetization (due to protons on the NaDNA) but less than the slowly relaxing component (from protons on the water molecules); therefore, only the water magnetization was inverted. At 40 MHz the monitor pulses of the T_1 r.f. sequence were "hard" and the nonselective and selective sequences are designated h-h and s-h, respectively. Therefore, at 40 MHz, all magnetization subsequent to the r.f. excitation was observed. At 200 MHz the monitor pulse was also a soft pulse; therefore, only the magnetization components decaying with long T_2 were observed; this pulse sequence is designated s-s. All NMR parameters were measured with the NaDNA fiber axis oriented at an angle of 54° with respect to the external magnetic field $\mathbf{B}_o$ (the magic angle); the T_2 and h-h T_1 measurements were also made with the fiber axis oriented parallel to $\mathbf{B}_o$.

RESULTS

The results of the spin grouping are presented in Table 1. The apparent spin relaxation is similar for both the 33% and 49% r.h. hydration samples. The magnetization fractions and the spin–spin relaxation times of the solid-like magnetization component ($T_2 \sim 13$ μs) and the semi-solid component ($T_2 \gtrsim 500$ μs), at both high field and in the rotating frame, agree with measurements of the free induction decay (FID) subsequent to a hard $\pi/2$ pulse. The solid magnetization component is characterized by a Gaussian line shape; using the convention of Kubo and Tomita (14), the T_2 is the time taken from the magnetization to decay to half its maximum value. In this convention the second moment (in gauss squared) for the solid magnetization is given by $M_2 = 1936/T_2^2$ (for T_2 in microseconds). Previous experiments on samples with $T_2 \sim 11$ μs (15) have confirmed that FID measurements with our spectrometers yield results identical to those of dipolar echo measurements which refocus the solid part of the magnetization lost in the receiver deadtime. The slower relaxing magnetization decayed exponentially and is termed the semi-solid component. The true T_2's of this magnetization, as measured by $\pi/2$-τ-π spin echo experiments, were 900 ± 100 μs and 2.5 ± 0.5 ms for the 33 and 49% r.h. samples, respectively (16, 17). Thus, the T_2 of the slowly decaying magnetization in the FID is not shortened significantly by macroscopic magnetic field homogeneities, hence the label semi-solid. It should be noted that the two components of the FID are well resolved because their T_2's differ by a factor of more than five (8). The magnetization fractions of the solid-like and semi-solid magnetiza-

TABLE 1 The apparent proton relaxation parameters for the hydrated NaDNA as determined by the spin-grouping experiments

Relative humidity		33%			49%		
Spin fraction (%)	H_2O	35 (37 ± 2)			47 (45 ± 2)		
	DNA	65 (63 ± 3)			53 (55 ± 3)		
		High fields results (hard-hard pulse sequence)					
Proton frequency		T_{1i}	T_{2i}	M_{oi}	T_{1i}	T_{2i}	M_{oi}
MHz		*ms*	*μs*	*%*	*ms*	*μs*	*%*
40		82 ± 2	434 ± 45	36 ± 3	86 ± 5	880 ± 100	47 ± 2
			13 ± 2	64 ± 3		13 ± 1	53 ± 2
200		370 ± 18	600 ± 60	35 ± 3	314 ± 16	655 ± 66	45 ± 4
			14 ± 2	65 ± 3		14 ± 1	55 ± 4
		High fields results (selective pulse sequence)					
		T_{1i}	T_{2i}	M_{oi}	T_{1i}	T_{2i}	M_{oi}
		ms	*μs*	*%*	*ms*	*μs*	*%*
40		82 ± 2	500 ± 50	19 ± 2	85 ± 2	724 ± 70	16 ± 2
			14 ± 2	37 ± 4		16 ± 2	32 ± 4
		8 ± 1	606 ± 61	24 ± 2	14 ± 2	1,000 ± 100	36 ± 2
			13 ± 2	−20 ± 3		15 ± 2	−17 ± 3
200		410 ± 50	—	—	333 ± 30	—	—
		10 ± 2	—	—	22 ± 3	—	—
		Rotating frame results (hard-hard pulse sequence)					
		$T_{1\rho i}$	T_{2i}	M_{oi}	$T_{1\rho i}$	T_{2i}	M_{oi}
		ms	*μs*	*%*	*ms*	*μs*	*%*
40 (and B_1 = 7G)		4.9 ± 0.4	13 ± 2	50 ± 4	5.4 ± 0.6	14 ± 3	47 ± 3
		0.8 ± 0.1	460 ± 50	37 ± 2	0.9 ± 0.1	600 ± 60	45 ± 3
			20 ± 3	13 ± 4		17 ± 3	8 ± 2

The spin fractions were determined by sample stoichiometry and by FID measurements (in brackets).

tion components confirm the water contents of the samples calculated from their stoichiometry. The results of the FID measurements and of the h-h T_1 spin groupings were independent of sample orientation for both low hydrations studied.

As shown in Fig. 1 *a*, the apparent spin-lattice recoveries at high fields are mono-exponential when measured with the nonselective inversion pulse sequence; that is, they are well characterized by single relaxation times. However, when the spin-lattice relaxation is measured with the selective inversion pulse sequence at high fields, it is characterized by two time constants. The magnetization decay in the rotating frame is also characterized by two spin-lattice relaxation times (see Fig. 1 *b*). In both samples the spin-grouping results show that the magnetization corresponding to the component relaxing with the short $T_{1\rho}$ of ~1 ms is the sum of solid and semi-solid FID's whereas the magnetization component relaxing with $T_{1\rho}$ ~ 5 ms is characterized by a solid-like T_2 only (see Fig. 2). Again the two components of the magnetization evolution seen in the selective inversion high field measurements and in the rotating frame measurements are well resolved because their relaxation times differ by at least a factor of five (8). The magnetization fractions observed in the rotating frame have been corrected for coupling of the Zeeman reservoir to the dipolar reservoir of the protons in the strong dipolar fields of the rigid lattice (18).

The results of the 40 MHz selective inversion s-h spin-grouping for the 33% r.h. NaDNA are shown in Fig. 3. The magnetization transfer between the water spin group and the protons on the NaDNA matrix is dramatically indicated by the FID decomposition afforded by spin-grouping (Fig. 3 *b*); note the growth of magnetization corresponding to the signal which relaxes with the short T_1. The growth of magnetization for this component is indicated by a negative magnetization fraction in Table 1. The magnetization fractions and T_2's

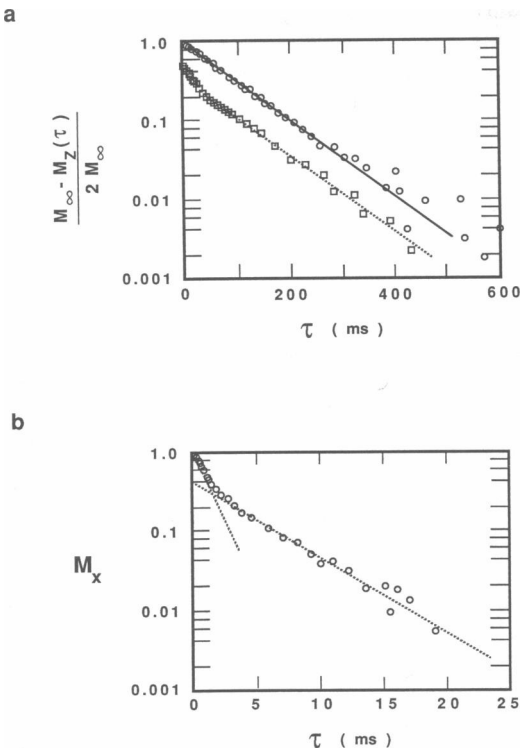

FIGURE 1 The magnetization evolutions from the 33% r.h. NaDNA T_1 and $T_{1\rho}$ experiments as recorded at a position 12 μs into the FID (the 12-μs window). The τ are the pulse spacings in the inversion recovery and the spin locking pulse sequences for the T_1 and $T_{1\rho}$ measurements, respectively. The magnetizations are in arbitrary units. (*a*) The circles (○) give the magnetization recovery subsequent to the nonselective h-h pulse sequence; it is characterized by a single apparent relaxation time of 82 ± 2 ms. The squares (□) show the recovery subsequent to the selective s-h pulse sequence which is characterized by two T_1's: 8 ± 1 and 82 ± 2 ms. (*b*) The magnetization decay in the rotating frame. It is characterized by two time constants: $T_{1\rho}$ = 4.9 ± 0.4 and 0.8 ± 0.1 ms.

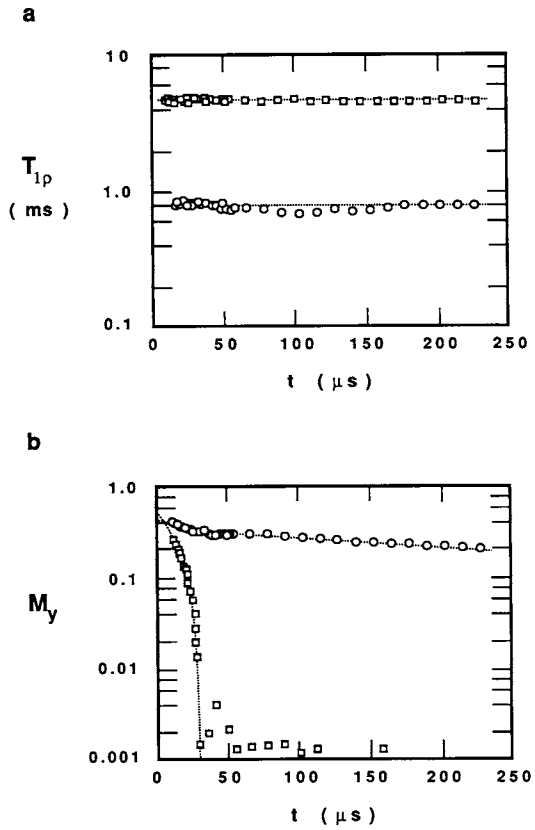

FIGURE 2 The results of the rotating frame spin-grouping experiments on the 33% r.h. NaDNA. (*a*) The variation of the measured $T_{1\rho}$'s with window position on the FID; the decay is characterized by two time constants at all positions on the FID. (*b*) The decomposed FID's corresponding to the two $T_{1\rho}$'s shown in *a*; the magnetizations are in arbitrary units. The magnetization characterized by the $T_{1\rho}$ ~4.9 ms (□) has an FID characteristic of a rigid solid with T_2 ~13 μs, the dashed line shows the Gaussian fit of the FID. The magnetization decaying with $T_{1\rho}$ ~0.8 ms has an FID characterized by both rigid solid like and semi-solid like T_2's of 20 and 460 μs, respectively. Note that the true apparent magnetization fractions of the signal decaying with the different spin-lattice relaxation times are determined only when the decomposed FID's are fitted and the zero-time intercepts are determined (6, 7).

corresponding to the decomposed FID's in the selective s-s spin-grouping at 200 MHz are not presented, as not all of the magnetization was monitored by the s-s sequence.

DISCUSSION

Effect of exchange on the apparent NMR relaxation of heterogeneous systems

The hydrated NaDNA is a heterogeneous system with the protons in at least two environments: one spin group consists of protons on water molecules and the other consists of protons on the DNA helix. The nuclear magnetic relaxation behavior of the system will be affected by exchange processes which occur between these spin groups (19, 20). Such exchange may involve the transfer of protons (chemical exchange involving labile protons on the hydrated macromolecule) or magnetization (dipolar exchange via spin flip-flops). The two-site exchange scenario is illustrated in Fig. 3. Note that the relaxation of the spin system is usually described in terms of relaxation rates in the analysis of exchange because it is the rates ($R_1 = T_1^{-1}, R_2 = T_2^{-1}, R_\rho = T_{1\rho}^{-1}$) which are additive.

In the absence of exchange processes, the observed (or apparent) spin relaxation is also the inherent relaxation behavior of the system; the observed (or apparent)

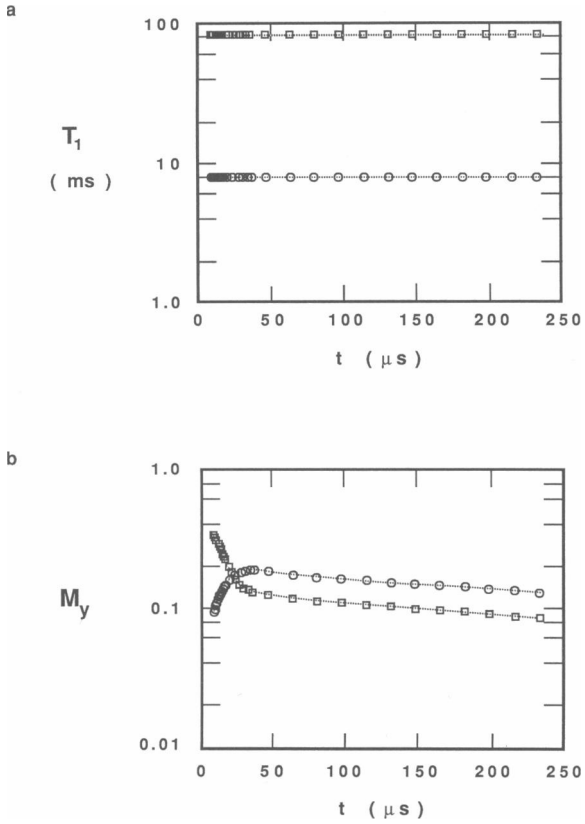

FIGURE 3 The results of the selective inversion s-h T_1 spin-grouping of the 33% r.h. NaDNA at 40 MHz. (*a*) The variation of the measured T_1's with window on the FID; the magnetization recovery is characterized by two time constants at all windows. (*b*) The decomposed FID's corresponding to the two T_1's shown in *a*. The growth of the magnetization component which relaxes with T_1 ~8 ms (○) is a manifestation of magnetization transfer from the hot water proton reservoir to the cold NaDNA spin group subsequent to the selective inversion pulse. The magnetization is in arbitrary units. Note: the magnetization evolution for the h-h spin-grouping is characterized by a single T_1 (~82 ms) at all windows. There is no additional decomposition of the FID possible with the h-h experiment.

magnetization fractions are the proton masses of the two spin groups; and the apparent relaxation rates are determined solely by the structure and dynamics of the individual spin groups. However, if exchange processes are present, the apparent relaxation parameters are no longer only functions of the inherent relaxation, but also depend on the exchange rates between the two spin groups. The relationship between the apparent and inherent relaxation parameters of the system and the exchange rates was first analyzed by Zimmerman and Brittin (19). The reduced magnetization, $m(\tau)$, evolves as

$$m(\tau) = C^+ e^{-\lambda^+ \tau} + C^- e^{-\lambda^- \tau}, \qquad (1)$$

where:

$$m(\tau) = \frac{m_o - m_z(\tau)}{2\, m_o} \text{ for inversion recovery } T_1, \qquad (2a)$$

$$m(\tau) = \frac{m_y(\tau)}{m_o} \text{ for } T_2, \text{ and} \qquad (2b)$$

$$m(\tau) = \frac{m_x(\tau)}{m_o} \text{ for } T_{1\rho}. \qquad (2c)$$

The apparent rates, λ^+ and λ^-, and the apparent magnetization fractions, C^+ and C^-, are given by:

$$\lambda^{\pm} = \tfrac{1}{2}\{(R_a + R_b + k_a + k_b) \pm [(R_a - R_b + k_a - k_b)^2 + 4k_a k_b]^{1/2}\}, \text{ and} \qquad (3)$$

$$C^{\pm} = p_a C_a^{\pm} + p_b C_b^{\pm} \text{ with} \qquad (4)$$

$$p_i C_i^{\pm} = \frac{\pm(R_i - \lambda^{\mp})}{\lambda_+ - \lambda^-} p_i m_i(0) \pm \frac{k_i}{\lambda^+ - \lambda^-} \cdot p_i \{m_i(0) - m_j(0)\}; {}^{j=a,b}_{j=b,a}. \qquad (5)$$

The R_a, R_b, p_a, and p_b are the inherent relaxation rates and magnetization fractions of the two spin groups, respectively, and the k_a and k_b are the exchange rates between the two groups (see Fig. 3). The $m_{i,j}(0)$ are the reduced magnetizations immediately following the r.f. pulse sequence. In the derivation of Eqs. 3–5, the condition of detailed balance, $p_a k_a = p_b k_b$, has been imposed. The dependence of the apparent relaxation parameters on exchange rate is illustrated in Fig. 4. Note that under slow exchange, with k_a, $k_b \ll R_a$ and R_b, the apparent relaxation parameters characterizing the system are equal to the inherent parameters; assuming $R_a > R_b$, then:

$$\lambda^+ = R_a, \lambda^- = R_b; C^+ = p_a, \text{ and } C^- = p_b. \qquad (6)$$

As the exchange rate increases, the apparent rates increase relative to the inherent rates; that is, the relaxation is observed to be faster than that of the uncoupled system, and the apparent magnetization fractions are no longer simply proportional to the sizes of the spin groups. As the exchange rate increases further to the so-called fast-exchange limit, the apparent relaxation of the system is simplified. The magnetization fraction corresponding to the fast relaxation rate vanishes quickly, and the relaxation is characterized by a single rate, λ^-, which is the weighted average of the inherent rates of the two spin groups, i.e.:

$$\lambda^- = p_a R_a + p_b R_b. \qquad (7)$$

Zimmerman and Brittin (19) pointed out that the

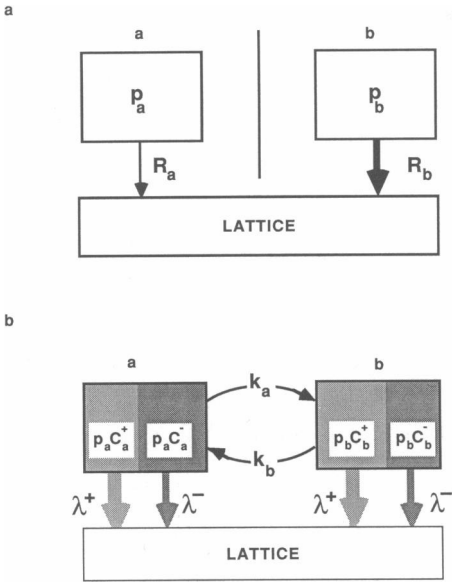

FIGURE 4 The spin relaxation parameters of a two site system with and without exchange processes present. (*a*) If there is no exchange between the 'a' and 'b' spin groups then the observed spin relaxation is the inherent relaxation. The fraction of protons in each group is given by the magnetization fractions p_a and p_b. The inherent relaxation rates R_a and R_b are determined only by the structure and dynamics of the two isolated groups. (*b*) However, if there is exchange between the two groups then the system is observed to relax with the apparent relaxation rates λ^+ and λ^- which are determined not only by the inherent rates, but also by the exchange rates between the two groups: k_a and k_b. The apparent magnetization fractions, C^+ and C^-, corresponding to these relaxation rates no longer correspond directly to the proton masses of the two spin groups, but are also modulated by exchange. Each spin group has some of its magnetization evolving with both relaxation rates (see text).

fast-exchange limit occurs when

$$\frac{k_i}{p_b(R_a - R_b)} \gg 1. \tag{8}$$

Computer simultations in this laboratory have shown that exchange appears to be in the fast regime when the left hand side of Eq. 8 is greater than $\sim\sqrt{20}$. It should also be noted that, in the fast exchange limit, the large relaxation rate, λ^+, no longer depends on the inherent relaxation rates of the system; rather, it is a function only of the exchange rates:

$$\lambda_+ = k_a + k_b, \tag{9a}$$

which, with detailed balance, reduces to

$$\lambda^+ = \frac{k_a}{p_b} = \frac{k_b}{p_a}. \tag{9b}$$

The utility of this equation was first realized by Edzes and Samulski (10) in their development of the selective inversion pulse sequences for T_1 measurements; the measurement of λ^+ by the selective inversion s-h pulse sequence enables the direct determination of the exchange rate, if the inherent spin mass of the spin groups are known.

While it is instructive to review the development and general behavior of Eqs. 1–9, it is in fact the inverse equations, relating the inherent relaxation rates to the apparent rates, which are of greater interest. Such equations have been developed in parametric form; and the determination of inherent parameters from apparent ones has been through graphical rather than analytic techniques (4, 6, 9, 21). One form of the solution of the inherent rates is given by:

$$R_a = \tfrac{1}{2}\{(\lambda^+ + \lambda^-) \pm [(\lambda^+ - \lambda^-)^2 - 4k_a k_b]^{1/2}\} - k_a \tag{10}$$

and

$$R_b = (\lambda^+ + \lambda^-) - R_a - k_a - k_b. \tag{11}$$

It has been noted (4, 21, 22) that only one solution of Eq. 10 is physically meaningful. With the spin-grouping technique, in which the apparent magnetization fractions are accurately determined, it is possible to find this solution by equating the $C^{\pm}$ (given by Eqs. 4 and 5) with the observed magnetization fractions (4, 9). In fact, the additional information provided by the spin-grouping analysis enables the direct determination of the inherent rates of a system with the following relationship:

$$R_a = \frac{\{(\lambda^+ + \lambda^-)C^- + p_b\lambda^- - p_a\lambda^+ - k_a\}}{(p_b - p_a)} \tag{12}$$

the obvious requirement being that the stoichiometry of the system (i.e., p_a and p_b) is known (8). The results of the spin-grouping measurements of the low hydration NaDNA at high fields and in the rotating frame have been analyzed for exchange utilizing Eqs. 7–12.

Exchange in low hydration NaDNA

At high fields the hydrated NaDNA magnetization recovery subsequent to a nonselective h-h inversion recovery pulse sequence can be described by a single relaxation time. However, when the T_1 is measured with a selective inversion s-h sequence the evolution becomes bi-exponential (see Fig. 1 *a*). This is a clear indication that, at high fields, the protons on the NaDNA and on the water molecules are coupled sufficiently strongly that the spin-lattice relaxation is in the fast exchange regime (on the time scale of the $T_1 \sim 80$ ms). If the mono-exponential recovery of the magnetization was

due to an accidental similarity of the T_1's for the water proton and the NaDNA proton spin groups, then the magnetization recoveries following the s-h selective inversion sequence would be characterized also by a single T_1, which it is not. From the results of the $T_{1\rho}$ spin grouping, it is clear that the exchange between the spin groups is not in the fast regime (on the time scale of $T_{1\rho} \sim$ 1–5 ms). Thus, the exchange analysis is strengthened by correlating the T_1 and $T_{1\rho}$ observations because the exchange is probed at two very different time scales. However, before the data from the two sets of experiments can be correlated, it is necessary to determine the exchange mechanism which is mixing the spin groups in the low hydration NaDNA.

Exchange mechanism in low hydration NaDNA

At the low hydration of these samples the water molecules are hydrogen bonded to the free oxygen atoms at the ionic phosphate site of the NaDNA helix backbone (13, 23). High resolution neutron quasi-elastic scattering (NQES) experiments indicate that (on a timescale of 10^{-10} s) the water does not diffuse freely at these hydrations and is localized at the phosphate group on the helix (24). Similar conclusions have been reached in computer simulations of hydrated NaDNA for hydration levels below six molecules of H_2O per nucleotide (25). Therefore, the water protons cannot chemically exchange with the labile protons on the helix because the only labile protons on the DNA helix are the NH and NH_2 hydrogens of the purine and prymidine bases. The only exchange process which can account for the magnetization transfer in the low hydration NaDNA is a dipolar exchange via mutual spin flips between the protons on the water molecules and the protons on the helix. This is an intergroup spin–spin flip–flop process. Therefore, with the low hydration NaDNA samples there is an exclusion of chemical exchange; this has been produced previously in nonaqueous systems (26, 27). It is important to carefully consider the dipolar exchange process because the dipolar Hamiltonian is diminished in the rotating frame and the spin–spin relaxation time in the rotating frame, $T_{2\rho}$, is twice the T_2 at high fields (28, 29). Therefore, exchange rates evaluated in the rotating frame, $k_{\rho i}$, (by the $T_{1\rho}$ spin-grouping and exchange analysis) and in the laboratory frame, k_i, (by the T_1 analysis) are related by:

$$k_i = 2k_{\rho i}. \tag{13}$$

This scaling has been incorporated in the high fields and rotating frame correlation analysis of the exchange dynamics.

Exchange analysis of the h-h T_1 results

The exchange analysis is simplified because the protons of the DNA spin group do not contribute significantly to the spin relaxation to the hydrated NaDNA. The DNA segmental motions are too slow to contribute significantly to the high fields relaxation (backbone $\tau_c > 5 \times 10^{-4}$ s [30]; base pairs $\tau_c > 10^{-4}$ s [31]); this is not expected to be changed by the addition of the water at low hydrations (32, 33). Thus, the relaxation of the DNA proton spin group is dominated by the reorientation of the CH_3 groups on the thymine bases. Because each CH_3 group must relax on average $\sim$42 other protons on the DNA helix, the relaxation rate of the DNA proton group is considered negligible (34) with a possible upper limit of $R_{DNA} \sim 2\ s^{-1}$ at 40 MHz. Measurements at 200 MHz on the 49% r.h. NaDNA sample hydrated with D_2O give the NaDNA proton relaxation rate of $\sim 0.1\ s^{-1}$ (35). Because $\omega_o\tau_c \gg 1$ for the NaDNA protons, R_{DNA} is approximately proportional to ω_o^{-2} and the upper limit for R_{DNA} at 40 MHz is $\sim 25 \times R_{DNA}$ at 200 MHz; i.e., $\sim 2.5\ s^{-1}$.

The spin-lattice relaxation at high fields is in the fast-exchange regime. Therefore, because the stoichiometry is well established and the relaxation rate of the DNA spin group known, it is possible to determine the inherent relaxation rate of the water protons, R_w, from Eq. 7 directly. The "a" and "b" spin groups correspond directly to the water and NaDNA proton groups. The relaxation rates of the water protons, as determined by the h-h spin grouping, are 33 and 6.7 s^{-1}, at 40 and 200 MHz, respectively ($T_{1W} \sim 33$ and ~ 150 ms). Thus, in agreement with studies of rehydrated lyophilized proteins (10, 22, 36), the water protons are the relaxation sink in the low hydration macromolecular system. Using Eq. 8, a lower limit to the exchange rate between the water and DNA proton groups can be calculated as $\sim 40\ s^{-1}$.

Incorporation of the s-s and s-h T_1 and the $T_{1\rho}$ exchange analysis

The additional information from the selective s-s and s-h T_1 and the $T_{1\rho}$ experiments can be used to determine more rigorously the inherent parameters of the different spin groups in the system. With spin-grouping, the magnetization decay in the rotating frame for both sample hydrations is characterized by two time constants of $\sim$1 and 5 ms. The FID corresponding to the magnetization which decays with the long $T_{1\rho}$ (i.e., having relaxation rate λ_ρ^-) is characteristic of a solid proton network only. The FID associated with the relaxation rate $\lambda_\rho^+ (T_{1\rho} \sim 1$ ms) is a sum of solid and semi-solid components; therefore, this magnetization component is due to both the NaDNA protons and the water protons.

In both low hydration samples, the apparent magnetization fraction associated with the fast relaxing magnetization, C_ρ^+, is larger than the spin mass of the water protons, p_W (in Table 1, C_ρ^+ is the sum of the magnetization fractions, M_{oi}, associated with $T_{1\rho} \sim 1$ ms). However, if the NaDNA and water protons were the two distinct spin groups undergoing exchange, C_ρ^+ would be less than the spin mass p_W because exchange between two spin groups will always reduce the apparent size of the magnetization having the larger relaxation rate (see Fig. 5). Therefore, the $T_{1\rho}$ spin-grouping results are a clear indication that the spin-lattice relaxation in the low hydration NaDNA cannot be modeled with a simple two-site exchange between the nucleotide protons and the water protons. Rather, there are some protons on the DNA helix which are coupled to the water protons so strongly that these protons, together with the water protons (H_2O protons), form a single spin group, hereafter designated the α spin group. These protons on the NaDNA helix are termed the α DNA spin group; the remainder of the NaDNA protons are termed the β DNA spin group. The β DNA protons are coupled to the α DNA protons via spin-diffusion through the DNA helix. The proposed model is illustrated in Fig. 6. Because the H_2O protons and the α DNA protons of the α spin group are coupled sufficiently strongly that they are in the fast exchange limit even on the time scale of the rotating frame spin-lattice relaxation times (~ 1 ms), the model for the relaxation is again a two site exchange model. However, the two spin groups (α and β) are no longer identified a priori with the water and DNA proton groups. To completely characterize the proton relaxation and exchange processes in the low hydration NaDNA, one must determine the inherent relaxation parameters of the three spin groups (the water protons, the α DNA protons, and the β DNA protons), the exchange between the α and β spin groups, and the exchange within the α group (that is between the α DNA spins and the water spins).

The inherent relaxation of the α and β spin groups can be calculated by using Eqs. 10–12. Because neither spin group can be identified stoichiometrically with the water nor the DNA protons, the spin masses of the α and β groups are not known. Therefore, a unique set of

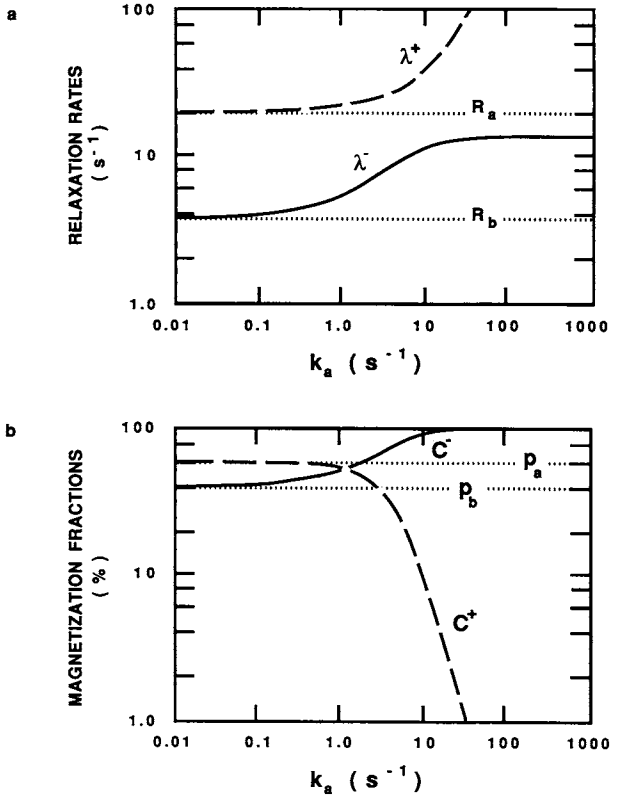

FIGURE 5 An illustration of the dependence of the apparent relaxation parameters in two site system on the exchange rate, k_a, between the two groups. (*a*) The dependence of the apparent relaxation rates on k_a. In the slow exchange regime ($k_a \ll R_a, R_b$) the apparent and inherent rates are equal. In the fast exchange limit the observed rate, λ^-, is the weighted average of the inherent rates. (*b*) The dependence of the apparent magnetization fractions on k_a: $C^\pm = p_a C_a^\pm + p_b C_b^\pm$. In the slow exchange limit the apparent and inherent fractions are identical. As the fast exchange limit is approached, the magnetization of the quickly relaxing component with the λ^+ rapidly vanishes, and all the magnetization relaxes with the rate λ^-. For the purpose of this illustration the inherent parameters have been set to: $R_a = 20\ s^{-1}$, $R_b = 3.7\ s^{-1}$, $p_a = 60\%$ and $p_b = 40\%$.

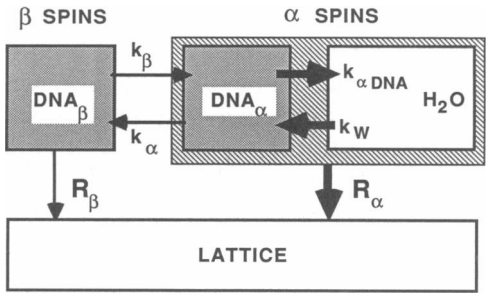

FIGURE 6 The inherent spin masses, relaxation rates, and exchange parameters in the proposed spin relaxation model for the low hydration NaDNA. The exchange rate between the water and the α DNA spins is sufficiently large that the whole α spin group can be regarded as one spin group in modeling both the high field and the rotating frame spin-lattice relaxation. The exchange rate between the α and β spin groups within the NaDNA proton environment is such that all spins relax in the fast exchange limit at high fields, while the exchange is not in the fast exchange regime in the rotating frame where the relaxation processes are faster. All the inherent parameters are given in Table 2.

inherent proton relaxation rates and exchange rates cannot be arrived at from the rotating frame results alone. For example, the apparent magnetization C_ρ^+ indicates only that p_α (the spin mass of the α DNA and the H_2O protons, together) must be >50% and 53% in the 33% and 49% r.h. NaDNA, respectively (see Table 1). However, adopting the general two-site exchange notation, one can plot the inherent proton relaxation and exchange rates which yield the observed apparent parameters as a function of an arbitrary spin mass, p_a. This is shown in Fig. 7 for the rotating frame spin-grouping of the 33% sample. Note that because the exchange rates must also satisfy the condition of detailed balance ($p_a k_{\rho a} = p_b k_{\rho b}$), the range of p_a for which the exchange analysis can reproduce the observed spin-grouping characterization of the spin-relaxation is very narrow ($35\% \leq p_a \leq 50\%$). Note also that the relaxation rate $R_{\rho b}$ is essentially independent of the spin masses of the different spin groups. Although the relaxation rate $R_{\rho a}$ depends strongly on the relative spin fractions of the two groups, it is determined uniquely once the true spin masses have been found. Therefore,

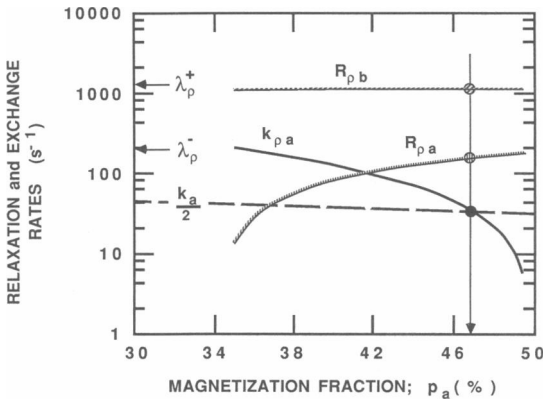

FIGURE 7 The solution loci for the inherent rates and exchange rates which yield the apparent relaxation observed with the $T_{1\rho}$ spin-grouping of the 33% r.h. NaDNA. The loci are determined with software (8) in which the general two site exchange parameters p_a and $k_{\rho a}$ are varied, and the inherent relaxation parameters giving the apparent relaxation are calculated using Eqs. 11 and 12. Each $k_{\rho a}$ for which physically realistic inherent relaxation rates can be calculated is plotted along with the corresponding inherent relaxation rates. Note that, because of the condition of detailed balance ($p_a k_{\rho a} = p_b k_{\rho b}$), realistic solutions exist over a narrow range of spin mass p_a only. The spin-grouping characterization of the apparent relaxation indicates clearly that the "a" spins of this diagram are identified with the β spin group of the model in Fig 6. The actual spin mass of the β group is determined by the intersection of the exchange rate found in the rotating frame exchange analysis with the scaled exchange rate determined from the λ^+ from the selective inversion s-h T_1 experiments. From this correlation analysis, $p_\beta = 47 \pm 4\%$.

the complete characterization of the inherent relaxation of the NaDNA follows directly once the "a" and "b" spin groups in Fig. 7 are identified, and the spin masses determined (see Table 2).

The association of the α or β spin groups with the "a" fraction of Fig. 7 is possible because of the complete characterization of the apparent spin-lattice relaxation by the spin-grouping technique. From spin-grouping the magnetization with the short $T_{1\rho}$ (the larger rate, $R_{\rho b}$, in Fig. 7) is identified unambiguously with the water protons because it is the only magnetization with a Lorentzian FID characterized by a T_2 of ~500 μs. Because the water protons contribute to the α spin magnetization, the spin group designated "b" in Fig. 7 corresponds to the α spin group.

The actual sizes of the α and β spin groups in the low hydration NaDNA can now be determined by correlating the results of the selective s-h and s-s high-fields spin-grouping and the rotating frame results. Since at high fields the α and β spin groups are in fast exchange, the short T_1 component of the s-h measurement is a direct measure of the exchange rate through Eq. 9. The T_1 exchange rate is plotted also versus spin mass in Fig. 7 taking into account that, when comparing the secular dipolar mixing exchange rates from the laboratory frame and the rotating frame, the exchange rates must be scaled, Eq. 13. The actual spin mass of the β spin group is given by the intersection of the two curves for the exchange rates as determined by the selective inversion T_1 measurements and the $T_{1\rho}$ measurements; that is, when $k_{\rho a} = k_a/2$. This occurs at p_β equal to 47 ± 3% and 44 ± 3% of the total proton mass for the 33% r.h. and the 49% r.h. NaDNA, respectively. As stated above, the inherent relaxation rates of the α and β spin groups and the exchange rates between the two groups are also determined uniquely by the intersection of $k_{\rho a}$ and $k_a/2$ in Fig. 7.

The β DNA protons are coupled to the α DNA protons via spin-diffusion through the DNA helix. The spin-diffusion is slow ($k_\beta \sim 50\ s^{-1}$, see Fig. 7 and Table 2) on the timescale of the $T_{1\rho}$ and represents a bottleneck in the relaxation of the system; i.e., it is the rate determining process for exchange between the α and β spin groups. That spin diffusion within the macromolecule could be the rate determining process for the exchange between water protons (or the protons on some small bound ligand) and the total biopolymer proton baths has been discussed previously (10, 26). Edzes and Samulski (10) estimated that spin-diffusion rate assuming that it would be comparable to the rate of spin flips in a rigid lattice (37), $W \sim [30\ T_2]^{-1} \sim 2 \times 10^3\ s^{-1}$ for NaDNa, although it was realized that this would be an upper limit in the rate due to the large interproton

TABLE 2 **The inherent proton relaxation characterization of the low hydration NaDNA**

Relative humidity		33%			49%		
		Spin masses (%)					
p_{DNA}		63 ± 3			55 ± 3		
p_W		37 ± 2			45 ± 2		
p_α		53 ± 4			56 ± 4		
p_β		47 ± 4			44 ± 3		
$p_{\alpha\,DNA}/p_{DNA}$		25 ± 4			20 ± 4		
p_W/p_α		70 ± 4			80 ± 5		
		Spin-lattice relaxation rates (s^{-1}) and times (ms)					
		High-fields		Rotating	High-fields		Rotating
		40 *MHz*	200 *MHz*	frame	40 *MHz*	200 *MHz*	frame
R_α		21 ± 2	5.0 ± 0.3	1,200 ± 160	19 ± 2	5.3 ± 0.3	1,100 ± 130
$[T_{1\alpha}]$		[47 ± 3]	[200 ± 20]	[0.83 ± 0.11]	[53 ± 4]	[190 ± 20]	[0.91 ± 0.11]
	$R_{\alpha DNA}$	$\lesssim 2$	~0.1	172 ± 25	$\lesssim 2$	~0.1	167 ± 27
	$[T_{1\alpha DNA}]$	[$\gtrsim$500]	[~5,000]	[5.8 ± 0.8]	[$\gtrsim$500]	[~5,000]	[6.2 ± 1.0]
	R_W	30 ± 3	7.1 ± 0.7	1,670 ± 220	24 ± 3	6.6 ± 0.6	1,300 ± 155
	$[T_{1W}]$	[33 ± 3]	[140 ± 15]	0.60 ± 0.08]	[42 ± 4]	[150 ± 16]	[0.77 ± 0.09]
R_β		$\lesssim 2$	~0.1	172 ± 25	$\lesssim 2$	~0.1	167 ± 27
		High fields exchange rates (s^{-1})					
k_α		57 ± 6			39 ± 7		
	$k_{\alpha\,DNA}$	>8,000 ± 1,600			>7,000 ± 1,400		
	k_W	>3,600 ± 800			>1,900 ± 450		
k_β		64 ± 7			49 ± 9		

The parameters are defined in the text and in Fig. 6. The characterization is derived by the correlation of the spin-grouping results and the FID measurements. See text for a discussion of the inherent rates for the NaDNA spin group. The exchange rates in the rotating frame are half those quoted for high fields.

distances which occur in macromolecules (26). With this estimate, it was considered that the macromolecular spin diffusion would not be the rate determining process in most situations. However, because spin diffusion is a random walk process (usually ~6 orders of magnitude less rapid than molecule diffusion), the spin-diffusion paths are expected to involve many spin flips and the rate of spin diffusion should be orders of magnitude slower than the spin-flip rate. The present estimate for the exchange rate within the macromolecule ($k_\beta \sim 50$ s^{-1}) indicates that such a spin-diffusion bottleneck exists in the NaDNA. Such a bottleneck has also been inferred from dipolar relaxation time (T_{1D}) measurements (38) on biopolymers. Because the stoichiometry of the hydrated NaDNA samples is well known, the proton fraction of the α DNA group, with respect to the total proton mass, can be calculated directly; $p_{\alpha DNA} = 16 \pm 2\%$ and 11 ± 2%, for the 33% r.h. and the 49% r.h. NaDNA, respectively; then $p_{\alpha NDA}/p_{DNA}$ is ~20–25% (see Table 2).

To characterize the inherent relaxation of the water protons in the rotating frame, the α spin group is analyzed further assuming fast exchange between the α DNA protons and the water protons using Eq. 7 written as $R_{\rho\alpha} = (p_W/p_\alpha)\, R_{\rho W} + (p_{\alpha DNA}/p_\alpha)\, R_{\rho\alpha DNA}$. The spin fractions are known; the water protons constitute the majority of the spins with $p_w/p_\alpha = 70 \pm 3$ and 80 ± 4% for the 33% r.h. and the 49% r.h. NaDNA, respectively. The α DNA relaxation rate is taken to be the same as that of the β protons determined in Fig. 7; that is, $R_{\rho\alpha DNA} = R_{\rho b} \sim 170\ s^{-1}$. The inherent spin-relaxation rate of the water protons in the rotating frame is ~1,500 s^{-1} for both NaDNA samples, see Table 2. The exchange rate within the α group can be estimated by the use of Eq. 8; $k_W >$ 2,000 s^{-1} (±20%) for both hydrations.

Incorporation of the T_2 exchange analysis

The assumption of fast exchange within the α spin group is tested by analysis of the spin–spin relaxation results

which are also moderated by the exchange processes (10, 19). The exchange rates within the α spin group ($k_W \sim 2{,}000\ s^{-1}$, see above) are sufficient that the spin–spin characterization of the magnetization corresponding to the $T_{1\rho} \sim 1$ ms component must be apparent (solid component with $\lambda_2^+ \sim 8\times 10^4\ s^{-1}$ and semi-solid component with $\lambda_2^- \sim 2{,}000\ s^{-1}$). The exchange analysis of the apparent T_2's indicates that on this time scale the exchange is actually in the intermediate regime, with an upper limit of $k_w \sim 1{,}500\ s^{-1}$. The spin–spin relaxation of the NaDNA (*solid*) magnetization is not significantly altered by the exchange; the inherent and apparent rates are identical ($R_{2DNA} = \lambda_2^+$), as are the inherent and apparent magnetization fractions. However, the T_2 of the water protons is long enough it is likely altered somewhat by the exchange. The inherent rate is slightly smaller than the observed rate (λ_2^-): $R_{2W} = 1{,}300 \pm 400\ s^{-1}$, and $1{,}100 \pm 400\ s^{-1}$ for the 33% and 49% r.h. samples, respectively. The error limits for R_{2W} reflect the range the smaller rate can take in the exchange analysis and still reproduce the observed apparent rates (recall the large range for $R_{\rho a}$ in Fig. 7). Although the T_2 analysis indicates that the α group is not internally in the fast exchange limit, the k_W from this analysis is not far below the limit predicted from the $T_{1\rho}$ results. Therefore, the approximation that the α spins act as a single spin group is very reasonable. This has been verified by a three site exchange analysis (39) of the low hydration NaDNA proton relaxation results (35).

Implications of neglecting cross-relaxation

A particular view of the exchange processes has been taken in the development of the relationships between the inherent and apparent relaxation parameters of a heterogeneous system, and in the interpretation of the exchange analysis. The magnetization of the two spin groups is considered to be mixed, in this particular case by mutual spin flips. In this approach the rates R_a and R_b are identified directly with the inherent relaxation rates of the *a* and *b* spin groups. In an alternate view of exchange via the dipolar interactions between the two spin groups, termed cross-relaxation (3, 10, 26, 36, 40), the mathematical development also leads to the equations of Zimmerman-Brittin (19), but the interpretation of the relaxation rates and of the exchange rates, k_a and k_b, is different. The rates R_i and k_i ($i = a, b$) are not considered to be only the respective inherent relaxation rates of the uncoupled spin groups and exchange rates; rather, they contain contributions from the spin-lattice relaxation due to the time-dependent dipolar interactions across the *a*/*b* interface. The dominant term of the cross-relaxation rate is dependent on the timescale at which the interactions at the interface take place. For example, in the case of a hydrated macromolecule the nature of the cross-relaxation depends on the correlation time of the water motion at the interface (3, 10). The existence of a cross-relaxation contribution to the spin-lattice relaxation at the macromolecule/water interface has been demonstrated previously (36, 41). However, the contribution of this intermolecular relaxation to total water relaxation rate ($33 \pm 8\ s^{-1}$) is less than the inherent relaxation of the uncoupled water spins ($25 \pm 4\ s^{-1}$) (36). Therefore, the view in which the exchange analysis gives the inherent relaxation rates of the water and NaDNA protons directly seems justifiable, and the subtraction of cross-relaxation contribution to the overall rate would not affect the results significantly within the errors of the analysis. The correlation times for the water dynamics from the model proposed below also support the view that dipolar mixing dominates the cross-relaxation. Isotope dilution studies are underway to better determine the contribution of cross-relaxation to the spin-lattice relaxation of the hydrated NaDNA.

Water dynamics in low hydration NaDNA

The determination of the inherent spin–spin and spin-lattice relaxation times of the water proton group enables one to model the dynamical behavior of the water molecules. Following previous studies of water motion in biopolymers at low hydrations (for example references 42 and 43), the spin-lattice relaxation is attributed to the intra-molecular relaxation associated with anisotropic motion of the water molecules. That the water motion in hydrated NaDNA is anisotropic has also been inferred previously from NMR measurements (16) which were interpreted as showing that the water molecules were oriented in the NaDNA matrix; however, the water dynamics were not modeled. The anisotropic water dynamics are characterized by two correlation times τ_r and τ_t which are associated respectively with the motion of the water molecule about the axis of rapid reorientation, and the slower tumbling of this fast reorientation axis. Because the NaDNA molecules in the oriented fibers are fixed, the slower motion of the reorientational axis is the "tumbling" of the water molecules only. The equations which relate the high field spin–spin and spin-lattice relaxation times to the anisotropic dynamics have been developed in the literature (22, 44) and are not quoted here. Following the derivation in references 22 and 44, $T_{1\rho}$ becomes:

$$T_{1\rho}^{-1} = \frac{1.1 \times 10^{-10}}{2} \cdot \{0.218\ \mathbf{D}(\tau_t) + 0.351\ \mathbf{D}(\tau_1) + 0.429\ \mathbf{D}(\tau_2)\}, \quad (14)$$

where 1.1×10^{10} s^{-2} is the coupling constant for water and the $\mathbf{D}(\tau_c)$ represent:

$$\mathbf{D}(\tau_c) = \left\{ \frac{3\tau_c}{1 + \omega_1^2\tau_c^2} + \frac{5\tau_c}{1 + \omega_0^2\tau_c^2} + \frac{2\tau_c}{1 + 4\omega_0^2\tau_c^2} \right\}. \quad (15)$$

The correlation times τ_1 and τ_2 are simple functions of the fast reorientation and the slow tumbling correlation times:

$$\tau_1^{-1} = \tau_t^{-1} + \tau_r^{-1} \quad (16a)$$

and

$$\tau_2^{-1} = \tau_t^{-1} + 4\tau_r^{-1}. \quad (16b)$$

The constants 0.218, 0.353, and 0.429 in Eq. 14 are determined from the orientation of the intra-proton vector to the axis of fast reorientation; the water is considered, in a first approximation, to have an equal probability of being oriented at either 90° or 38° (22).

It is possible to present the spin relaxation times due to the anisotropic dynamics in terms of one correlation time only because, at a fixed temperature, the two times τ_r and τ_t are related. The anisotropic motion of the water molecules is considered to be thermally activated so that both correlation times follow an Arrhenius temperature dependence. Although each correlation time τ_r and τ_t is specified by its own activation energy and correlation coefficient, the correlation times, and their ratio τ_t/τ_r, are fixed at a particular temperature; therefore, one can model the relaxation considering one correlation time only. The inherent relaxation times for the water molecules in the low hydration NaDNA agree well with those predicted by the anisotropic dynamics relaxation mechanism when τ_t/τ_r is in the range from ~100–300 (see Fig. 8 in which τ_t/τ_r has been set to 200). The measured inherent rates correlate well with $1.5 \times 10^{-7} \leq \tau_t \leq 8 \times 10^{-7}$ s. Thus, the tumbling of the water molecules in the low hydration NaDNA is about five orders of magnitude slower than in bulk water (cf. reference 45, where isotropic reorientation is characterized by a single correlation time τ_r of 2.7×10^{-12} s). The fast reorientation ($5 \times 10^{-10} \leq \tau_r \leq 8 \times 10^{-9}$ s) is about three orders of magnitude slower than in bulk water. The values of the tumbling and fast reorientation correlation times reported in this work have been confirmed by $T_{1\rho}$ dispersion measurements on low hydration NaDNa in which it has been found that the $T_{1\rho}$ of the water protons is nondispersive (35). These values for the correlation times also agree with those determined in studies on hydrated biopolymers with similar water contents (22, 43, 46).

It has been suggested that the anisotropic dynamics of water in hydrated systems should be represented by a distribution of correlation times for both the reorientation and tumbling motions (22). In the present system, however, the distributions must be quite narrow as the agreement of the measured inherent T_1, $T_{1\rho}$, and T_2 with the anisotropic reorientation model with a narrow range of τ_t and of τ_r is excellent. This is not surprising because, as discussed above, the water molecules in the low hydration NaDNA paracrystal are hydrogen bonded to identical sites on each nucleotide of the DNA duplex (13, 24–26).

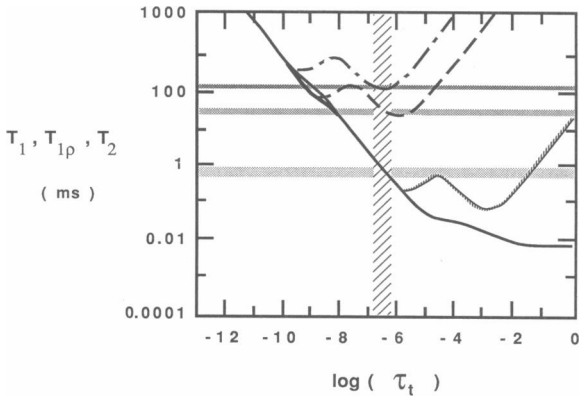

FIGURE 8 The modified BPP plot of the spin relaxation of the water protons under the assumption that the relaxation mechanism is anisotropic reorientation of the water molecules. The relaxation times are given as functions of the tumbling correlation time, τ_t; τ_t/τ_r has been set at 200 for the purpose of this illustration. The T_1 is calculated at ν_o = 40 and 200 MHz, and $T_{1\rho}$ at B_1 = 7 G. The observed inherent relaxation of the water protons in the 33% r.h. hydrated sample is indicated by the shaded regions; the corresponding range of τ_t by the cross-hatched bar.

CONCLUSIONS

In any heterogeneous material, the measured NMR relaxation parameters do not directly provide the inherent spin-relaxation times and magnetization fractions of the protons within the system. From the present study this is true for even the simplest of biological model systems: a hydrated macromolecule in the paracrystalline phase. However, the inherent relaxation of the various spin groups is tractable. A three step correlation analysis is proposed as a technique for the determination of molecular dynamical information from NMR experiments. The first step is the characterization of the observed spin-relaxation as completely as possible. This is achieved with the spin-grouping technique, through which the apparent spin-lattice and spin–spin relaxation behavior of the magnetization are readily correlated (7, 8). The second step is the exchange analysis of the

apparent relaxation using the Zimmerman-Brittin model for exchange modified relaxation (9, 19). This procedure is strengthened by the correlation of apparent spin-lattice relaxation at high fields with that in the rotating frame. Because the $T_{1\rho}$'s of model biological systems are typically one or two orders of magnitude less than their respective T_1's, the exchange analysis is made more reliable when the exchange is probed at both time scales. Additional information is obtained through the analysis of selective inversion T_1 spin-grouping results (10) and by the exchange analysis of the spin–spin relaxation. The complete correlation of the results of a number of different experiments ensure that the determination of the inherent spin-relaxation and of the exchange processes are indeed unique. Once this second step is completed, and the inherent relaxation parameters are uniquely determined, the molecular dynamics of the sample may be modeled.

The three stage NMR analysis is well illustrated in this study of water dynamics in low hydration paracrystals of NaDNA, which are ideal as a model system because the environment of the water molecules is well defined. This is not always the case for other model systems such as proteins hydrated from the gas phase (33). The low hydration NaDNA sample stoichiometry is well known (13) and, at the hydration levels studied, the water molecules are localized at the ionic phosphate site of the DNA backbone (13, 23, 24). Therefore, all water molecules are in equivalent sites in the macromolecule matrix (25). The implication of this for the analysis of the exchange processes, which strongly influence the proton relaxation of the system, is that the exchange between the NaDNA and the water protons is limited, a priori, to magnetization transfer due to dipolar mixing.

The inherent proton relaxation of the hydrated NaDNA supports previous findings of the high field spin-lattice relaxation of hydrated macromolecules (10, 22, 33, 36). For both the 33% and 49% r.h. samples the T_1 relaxation is in the fast exchange limit with the water proton group acting as the relaxation sink for the total spin bath. The inherent T_1 of the water protons is determined to be $\sim$30 and $\sim$145 ms at 40 and 200 MHz, respectively. As has been observed, for example, in tissues (4–6), the rotating frame spin-lattice relaxation is not in the fast exchange limit. However, the water protons are still the relaxation sink of the system with $T_{1\rho}$ $\sim$0.7 ms. The exchange across the water-macromolecule interface is very rapid ($k_{\alpha DNA} \sim 7{,}000\ s^{-1}$). About 25% of the protons on the macromolecule are in such intimate contact with the water protons that, together, they act as one spin-group. In the present study it has been found that the rate determining bottleneck in the relaxation of the total NaDNA-water spin bath is the slow spin-diffusion within the NaDNA ($k_\alpha \sim 50\ s^{-1}$). Although the determined spin-diffusion rate is strongly dependent on the structure of the NaDNa paracrystal, it suggests that previous estimates for the spin-diffusion rate within a macromolecule may have been overestimated by one or two orders of magnitude. The two site exchange model must be applied with care in the analysis of the proton relaxation of hydrated polymers as the two spin groups do not correspond directly with the water protons and the macromolecule protons.

The inherent T_1, $T_{1\rho}$, and T_2 of the water protons are consistent with those predicted with a model in which the water molecules undergo anisotropic reorientation. The correlation time for the fast reorientation of the water molecules about the hydrogen bond axis is $5 \times 10^{-10} \leq \tau_r \leq 8 \times 10^{-9}$ s. While τ_r is about three orders of magnitude slower than the correlation time for bulk water motion, the correlation time for the tumbling of the water molecules ($1.5 \times 10^{-7} \leq \tau_t \leq 8 \times 10^{-7}$ s) is about five orders of magnitude slower than that of bulk water. These values agree with previous estimates from hydrated macromolecular systems (22, 43, 46).

The three stages of spin-grouping, exchange analysis, and dynamical modeling outlined here are very useful in the elucidation of the NMR relaxation of molecular systems of biological interest. These same techniques are currently being applied to studies of a variety of mammalian tissues in an effort to correlate the dynamical information with tissue characterization by NMR imaging.

Received for publication 2 September 1988 and in final form 2 July 1990.

REFERENCES

1. Bottomly, P. A., T. H. Foster, R. E. Adersinger, and L. M. Pfiefer. 1984. A review of normal tissue hydrogen NMR relaxation times and relaxation mechanisms from 1–100 MHz: dependence on tissue type, NMR frequency, temperature, species, excision, and age. *Med. Phys.* 11:425–448.
2. Bottomly, P. A., C. J. Hardy, R. E. Adersinger, and G. Allen-Moore. 1987. A review of ^{1}H nuclear magnetic resonance relaxation in pathology, are T_1 and T_2 diagnostic? *Med. Phys.* 14:1–37.
3. Lynch, J. L. 1983. Water relaxation in heterogeneous and biological systems. *Magn. Reson.* 2:248–260.
4. Sobol, W. T., I. G. Cameron, W. R. Inch, and M. M. Pintar. 1986. Modeling of proton spin relaxation in muscle tissue using nuclear magnetic resonance spin grouping and exchange analysis. *Biophys. J.* 50:181–191.
5. Sridharan, K. R., L. J. Schreiner, D. W. Kydon, and M. M. Pintar. 1985. Characterization of normal and malignant mouse tissue by NMR lineshape-relaxation correlations in the rotating frame. *Magn. Reson. Med.* 2:73–80.
6. Sobol, W. T., and M. M. Pintar. 1987. NMR spectroscopy of

heterogeneous solid-liquid mixtures. Spin-grouping and exchange analysis of proton spin relaxation in tissue. *Magn. Reson. Med.* 4:537–554.

7. Peemoeller, H., and M. M. Pintar. 1980. Two-dimensional time-evolution approach for resolving a composite free-induction decay. *J. Magn. Reson.* 41:358–360.
8. Schreiner, L. J., and M. M. Pintar. 1985. NMR and neutron studies of water dynamics in dense solutions. *J. Physique.* C7:241–248.
9. Schreiner, L. J. 1985. Correlation approach in Nuclear Magnetic Resonance: application to hydrated NaDNA. Ph.D. thesis. University of Waterloo, Ontario, Canada. 185 pp.
10. Edzes, H. T., and E. T. Samulski. 1978. The measurement of cross-relaxation effects in the proton NMR spin-lattice relaxation of water in biological systems: hydrated collagen and muscle. *J. Magn. Reson.* 31:207–229.
11. Rupprecht, A. 1970. A wet spinning apparatus and auxiliary equipment suitable for preparing samples of oriented DNA. *Biotechnol. Bioeng.* 12:93–121.
12. Rupprecht, A., and B. Forslind. 1970. Variation of electrolyte content in wet-spun lithium- and sodium-DNA. *Biochim. Biophys. Acta.* 204:304–316.
13. Falk, M., K. A. Hartman, and R. C. Lord. 1962. Hydration of deoxyribonucleic acid. I. A gravimetric study. *J. Am. Chem. Soc.* 85:3843–3846.
14. Funduk, N., D. W. Kydon, L. J. Schreiner, H. Peemoeller, L. Miljkovic, and M. M. Pintar. 1984. Composition and relaxation of the proton magnetization of human enamel and its contribution to the tooth NMR image. *Magn. Reson. Med* 1:66–75.
15. Kubo, R., and K. Tomita. 1951. A general theory of magnetic resonance absorption. *J. Phys. Soc. Jpn.* 9:888–919.
16. Lahajnar, G., I. Zupancic, L. J. Miljkovic, and A. Rupprecht. 1978. The structure of water sorbed in oriented DNA samples. *Period. Biol.* 80:135–140.
17. Miljkovic, L. J. 1979. Istrazivanje moiekulske strukture i dinamike bioloskih makromolekula i tekucih kristala sa nuklearnom magnetnom rezonancijom. Ph.D. thesis. University of Nis, Yugoslavia.
18. Goldman, M. 1970. Spin Temperature and Nuclear Magnetic Resonance in Solids. Oxford University Press, U.K. 48–74.
19. Zimmerman, J. R., and W. E. Brittin. 1957. Nuclear magnetic resonance studies in multiple phase systems: lifetime of a water molecule in an absorbing phase on silica gel. *J. Phys. Chem.* 61:1328–1333.
20. Woessner, D. E. 1961. Nuclear transfer effects in nuclear magnetic resonance pulse experiments. *J. Chem. Phys.* 35:41–48.
21. Winkler, H., and A. Gutsze. 1981. On two-component NMR relaxation. *Adv. Mol. Relax. Interact Processes.* 21:159–179.
22. Shirley, W. M., and R. G. Bryant. 1982. Proton-nuclear spin-relaxation and molecular dynamics in the lysozyme-water system. *J. Am. Chem. Soc.* 104:2910–2918.
23. Mrevlishvili, G. M. 1977. Thermodynamic properties of biopolymers in the helical and coiled state in the temperature interval 4–400°K. *Biophysica (Russ.)* 22:180–191.
24. Schreiner, L. J., M. M. Pintar, A. J. Dianoux, F. Volino, and A. Rupprecht. 1988. Hydration of NaDNA by neutron quasi-elastic scattering. *Biophys. J.* 53:119–122.
25. Clementi, E. 1986. Simulations of complex chamical systems. *Methods Enzymol.* 127:114–140.
26. Andree, P. J. 1978. The effect of cross relaxation on the longitudinal relaxation times of small ligands binding to macromolecules. *J. Magn. Reson.* 29:419–431.
27. Bryant, R. G., and M. Jarvis. 1984. Nuclear magnetic relaxation dispersion in protein solutions. A test of proton-exchange coupling. *J. Phys. Chem.* 88:1323–1324.
28. Barnaal, D., and I. J. Lowe. 1963. Effects of rotating magnetic fields on the free-induction decay shapes. *Phys. Rev. Lett.* 11:258–260.
29. Jones, G. P. 1966. Spin-lattice relaxation in the rotating frame: weak collision case. *Phys. Rev.* 148:332–335.
30. Nall, B. T., W. P. Rothwell, J. S. Waugh, and A. Rupprect. 1981. Structural studies of A-form sodium deoxyribonucleisc acid: phosphorus-31 nuclear magnetic resonance of oriented fibres. *Biochemistry.* 20:1881–1887.
31. DiVerdi, J. A., and S. J. Opella. 1982. N-H bond lengths in DNA. *J. Am. Chem. Soc.* 104:1761–1762.
32. Andrew, E. R., D. J. Bryant, and T. Z. Rizvi. 1983. The role of water in the dynamics and proton relaxation of solid proteins. *Chem. Phys. Lett.* 95:463–466.
33. Bryant, R. G., and W. M. Shirley. 1980. Dynamical deductions from nuclear magnetic relaxation measurements at the water-protein interface. *Biophys. J.* 32:3–16.
34. Andrew, E. R., T. J. Green, and M. J. R. Hoch. 1978. Solid-state proton relaxation of biomolecular components. *J. Magn. Reson.* 29:331–339.
35. MacTavish, J. C. 1988. The NMR characterization of water in NaDNA paracrystals. Ph.D. thesis. University of Waterloo, Ontario, Canada.
36. Peemoeller, H., D. W. Kydon, A. R. Sharp, and L. J. Schreiner. 1984. Cross relaxation at the lysozyme-water interface: an NMR line-shape-relaxation correlation study. *Can. J. Phys.* 62:1002–1009.
37. Abragam, A. 1961. Principles of Nuclear Magnetism. Oxford University Press, U.K. 97–158.
38. Gaspar, R., E. R. Andrew, D. J. Bryant, and E. M. Cashell. 1982. Dipolar relaxation and slow molecular motions in solid proteins. *Chem. Phys. Lett.* 86:327–330.
39. Eisenstadt, M. 1980. NMR hybrid relaxation methods of studying chemical, physical, and spin exchange: I. General theory and experimental methods. *J. Magn. Reson.* 38:507–527.
40. Solomon, I. 1955. Relaxation processes in a system of two spins. *Phys. Rev.* 99:59–565.
41. Fund, B. M., and T. W. McGaughy. 1980. Cross-relaxation in hydrated collagen. *J. Magn. Reson.* 39:413–420.
42. Borah, B., and R. G. Bryant. 1982. Deuterium NMR of water in immobilized protein systems. *Biophys. J.* 38:47–52.
43. Peemoeller, H., F. G. Yeomans, D. W. Kydon, and A. R. Sharp. 1986. Water molecule dynamics in hydrated lysozyme: a deuteron magnetic resonance study. *Biophys. J.* 49:943–948.
44. Woessner, D. E. 1962. Spin relaxation processes in two-proton system undergoing anisotropic reorientation. *J. Chem. Phys.* 36:1–4.
45. Glasel, J. A. 1978. Water: a Comprehensive Treatise. F. Franks, editor. Plenum Press, New York. 215–254.
46. Wong, T. C., and T. T. Ang. 1985. Study of molecular dynamics of water adsorbed on macroscopically oriented cellulose by deuteron nuclear magnetic relaxation. *J. Phys. Chem.* 89:4047–4051.